Available online at www.sciencedirect.com

ScienceDirect

Energy Procedia 105 (2017) 738 – 743

Energy Procedia

The 8th International Conference on Applied Energy – ICAE2016

Urban Integration of Aeroelastic Belt for Low-Energy Wind Harvesting

Angelo I. Aquino*, John Kaiser Calautit, Ben Richard Hughes

Department of Mechanical Engineering, University of Sheffield, Sheffield S10 2TN, UK

Abstract

In this modern age low-energy devices are pervasive especially when considering their applications in the built-environment. The multitude of low-energy applications extend from wireless sensors, radio-frequency transceivers, charging devices, cameras and other small-scale electronic devices. The energy consumptions of these devices range in the milliwatt and microwatt scale which is a result of continuous development of these technologies. Thus, renewable wind energy harnessed from the aeroelastic effect can play a pivotal role in providing sufficient power for extended operation with little or no battery replacement. An aeroelastic belt is a simple device composed of a tensioned membrane coupled to electromagnetic coils and power conditioning components. This simplicity of the aeroelastic belt translates to its low cost and overall modularity. The aim of this study is to investigate the potential of integrating the aeroelastic belt into the built environment using Computational Fluid Dynamics (CFD) simulations. The work will investigate the effect of various external conditions (wind speed, wind direction and physical parameters, positioning and sizing) on the performance of the aeroelastic belt. The results from this study can be used for the design and integration of low-energy wind generation technologies into buildings.

Peer-review under responsibility of the scientific committee of the 8th International Conference on Applied Energy.

Keywords: Airflow; Aeroelastic flutter; Buildings; Computational Fluid Dynamics (CFD); Simulation; Wind; Wind belt

1. Introduction

Buildings account for 20-40% of total energy consumption in developed countries, which is a figure higher than the consumptions of industry and transport sectors [1]. One major benefit of developing wind energy harvesting in buildings is the obvious - bringing the power plant closer to the power consumers. Due to distribution of power creation capabilities to the public, people can expect higher energy efficiency, reduced dependence to energy companies, lower carbon footprint and overall stimulation of the economy [2]. Add to the aforementioned, distributed power creation will significantly decrease the load of the grid, dependence on diesel generators (in events of power outage) and power transmission costs.

*Corresponding author. Tel.: +447513-259-309
E-mail address: choloaquino@gmail.com.

Peer-review under responsibility of the scientific committee of the 8th International Conference on Applied Energy.
doi:10.1016/j.egypro.2017.03.384

On the observation of numerous past literature, there have been no prior studies regarding the intelligent placement of the aeroelastic belt in built environments. In particular, research using Computational Fluid Dynamics (CFD) to optimise this energy harvester's installation has been minimal. This research gap is therefore addressed in this study and is a new and different approach in aeroelastic belt research.

Previous studies about the building environment's potential for wind energy harvesting highlighted the need for sensible analysis of wind flow around buildings. To utilise the effect of wind acceleration above or around buildings and to determine the proper types of wind energy technologies, analyses of positions of wind energy harvesters have to contain more information that can result to better decisions [2]. This present study is a novel step towards integration of the aeroelastic belt into buildings [3]. We emphasise the significance of using CFD which can be used to optimise location before conducting field experiments to obtain the actual performance. In the case of this investigation, the main objective is to identify areas of a given building that maximise speeding-up which translates to maximising energy harvested, given three different cases for wind directions (0˚, 45 ˚ and 90˚).

2. Literature Review and Objectives

One of incipient technologies with respect to low-energy wind harnessing is the group regarded as "flutter-based" energy harvesters. These devices stand as alternatives to conventional wind turbines and have certain advantages in terms of the absence of constituent moving parts, leading to reduced production costs and longer system lifespan. Important to note as well that flutter-based wind energy can even be designed to adapt to highly fluctuating wind speeds and directions [4].

In order to increase the lifecycles of Wireless Sensor Networks (WSN), continuous research is being conducted in terms of alternative power sources that are appropriate for their scale. WSN technologies are currently deployed in the milliwatt and microwatt range of power consumption [5]. This can be perceived as an attractive and lucrative niche for small-scale energy harvesters, most notably the type we now consider as the aeroelastic belt. This wind energy harvester uses aeroelastic flutter to convert the kinetic energy transmitted by the wind into electrical energy. The current study focuses on CFD simulations on installations of the aeroelastic belt on different exterior regions of a building, using a cut-in wind speed of 3 m/s as specified by the device manufacturer as seen in [6], with the main objective of contributing to the decision-making when it comes to real applications.

The work will investigate the effect of various external conditions and device locations on the performance of the aeroelastic belt. The simulation will use a gable-roof type building model with a 27˚ pitch as shown in Fig. 1a. The atmospheric boundary layer (ABL) flow will be used for the simulation of the approach wind. The 3-D Reynolds-averaged Navier-Stokes (RANS) equations along with the momentum and continuity equations will be solved using ANSYS FLUENT 16 for obtaining the velocity and pressure field. Sensitivity analyses for the grid resolutions of the CFD simulations will be performed for verification of modelling. The results of the flow around the buildings and surface pressure coefficients will be validated with previous experimental work. The study will use regression analysis and experimental data [4] to estimate the power output of the aeroelastic belt. The coil used in the transducer is made of 38 awg enamel coated wire with approximately 150 turns and resistance of approximately 25 ohms [7]. Fig. 1a shows the location of the aeroelastic belt around the building geometry.

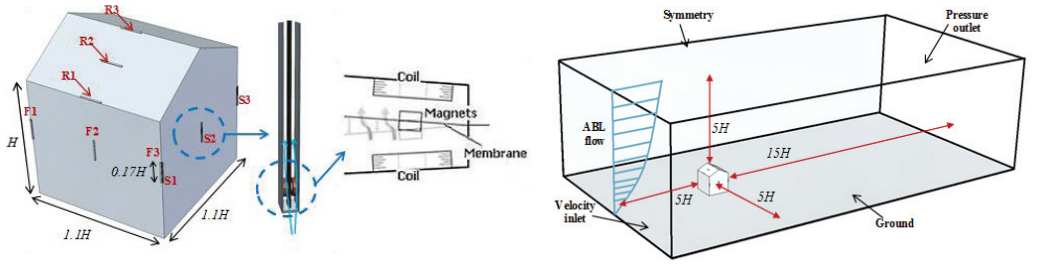

Fig. 1 (a) CAD geometry of building with aeroelastic belt devices; (b) computational domain of building with aeroelastic belt devices

3. Research Methodology

3.1 Computational Fluid Dynamics (CFD) modelling

The basic assumptions for the numerical simulation include a three-dimensional, fully turbulent, and incompressible flow. The flow was modelled by using the standard k–e turbulence model, which is a well-established method in research on wind flows around buildings [8, 9]. The CFD code was used with the Finite Volume Method (FVM) approach and the Semi-Implicit Method for Pressure-Linked Equations (SIMPLE) velocity-pressure coupling algorithm with the second order upwind discretisation. The general governing equations include the continuity, momentum and energy balance for each individual phase. The standard k-e transport model was used to define the turbulence kinetic energy and flow dissipation rate within the model. The governing equations together with the transport equations also utilised in ANSYS Fluent.

Computational domain. The geometry (Fig. 1a) was created using commercial CAD software and then imported into ANSYS Geometry (pre-processor) to create a computational model. The shape of the building was based on [9], which is a gable roof type building with a roof pitch of 26.6°. The overall dimension of the building was 3.3m (L) x 3.3m (W) x 3m (H). To create a computational domain, the fluid volume was extracted from the solid mode. The fluid domain consisted of an inlet on one side of the domain and an outlet on the opposing boundary wall. The computational domain size and location of model were based on the guideline of COST 732 [9] for environmental wind flow studies. According to the guidelines, for a single building with the height H, the horizontal distance between the sidewalls of the building and side boundaries of the computational domain should be 5H. Similarly, the vertical distance between the roof and the top of domain should also be 5H. In the flow direction, the distance between the inlet and the façade of the building should be 5H while for the leeward side and outlet, it should be 15H to allow the flow to re-develop behind the wake region, as fully developed flow is normally assumed as the boundary condition in steady RANS calculations [9].

Computational grid and sensitivity analysis. Due to the complexity of the model, a non-uniform mesh was applied to volume and surfaces of the computational domain. The generated computational mesh of the building model is shown in Fig. 1b. The grid was modified and refined according to the critical areas of interests in the simulation such as the aeroelastic belt. The size of the mesh element was extended smoothly to resolve the areas with high gradient mesh and to improve the accuracy of the results. The inflation parameters were set according to the complexity of the geometry face elements, in order to generate a finely resolved mesh normal to the wall and coarse parallel to it. Sensitivity analysis was used to verify the computational modelling of the building integrated with the aeroelastic belt. The computational grid was based on a sensitivity analysis which was performed by conducting additional simulations with same domain and boundary conditions but with various gird sizes. The process increased the number of elements between 2.44 (coarse) and 4.90 million (fine). The average value of the airflow velocity in the vertical line in the R1 belt was used as the error indicator. The maximum error between the fine and medium mesh was 3.4% or ±0.08m/s while the average was 1%. Thus, the repetition of numerical model with finer mesh had no considerable effects on the results.

Boundary conditions. The boundary conditions were specified according to the AIJ guidelines [9]. The profiles of the airflow velocity U and turbulent kinetic energy (TKE) were imposed at the inlet which were based on [9], with the stream-wise velocity of the approaching flow obeying the power law with an

exponent of 0.25 which corresponds to a sub-urban terrain. The values of ε for the k-epsilon turbulence model were acquired by assuming local equilibrium of $Pk = \varepsilon$ [9]. The standard wall functions were applied to the wall boundaries except for the ground, which had its wall functions adjusted for roughness. The horizontal non homogeneity of the ABL was limited by adapting sand-grain roughness height and roughness constant to the inlet profiles, following the equation of [9]: $k_s=9.79z_0/c_s$; where z_0 is the aerodynamic roughness length of the sub-urban terrain. The values selected for sand-grain roughness height and a roughness constant 1.0 mm and 1.0 [9]. The sides and the top of the domain were set as symmetry. For the outlet boundary, zero static pressure was used.

3.2 Estimation of wind power

The study utilised regression analysis using a polynomial curve of degree three to extrapolate power output given integral-value wind speed. Experimental data from [3] was used, with varying wind speed and the corresponding output power, using the optimal load and tension for an aeroelastic belt. A degree three polynomial is analogous to the fundamental equation for wind power making the choice for this polynomial type more sensible. Regression analysis was able to obtain an R-squared value of 0.9666. Using the manufacturer's specifications [3], cut-in wind speed is limited to 3 m/s. Therefore in order to extract results using the same aeroelastic belt, reconfiguration of the belt has to be done on installations on areas of the buildings with wind speeds lower than 3 m/s. This investigation simulated a gentle breeze, which is category 3 in the Beaufort wind force scale.

4. Method Validation

Figures 2a and b show a comparison between the experimental PIV results of [9] and the current modelling results of the velocity distribution around the building model. The results of the airflow velocity close to the windward wall seem to be at a lower speed in the model compared to the PIV results, however a similar pattern was observed for most areas particularly close to the roof. Fig. 2c and d show a comparison between the prediction of the current model and [9] of the pressure coefficient distribution around the building model.

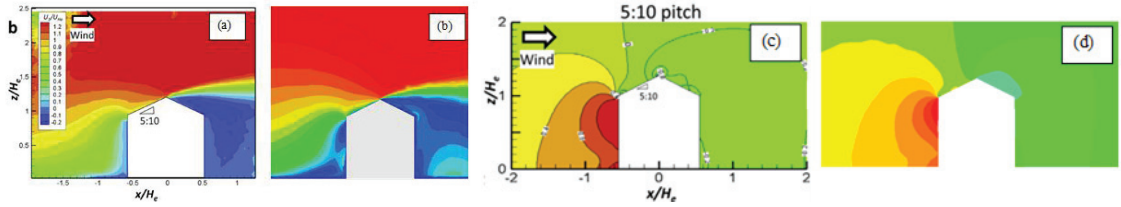

Fig. 2. (a) PIV measurements of velocity [9] (b) velocity distribution in the current model (c) pressure coefficient result [9] (d) pressure coefficient distribution in the current model.

4. Results and Discussions

Fig. 3a shows the velocity contours of a side view cross-sectional plane inside the computational domain representing the airflow distribution around the building integrated with aeroelastic belt. As observed, the approach wind profile entered from the right side of the domain and the airflow slowed down as it approached the building and lifted up. Separation zones were observed on the lower windward side of the building and also at the leeward side of the building and roof. Zoomed in views of the velocity distribution around the aeroelastic belt R1, R2 and R3 are shown on top of the diagram. The results show that the shape and angle of the roof can have a significant impact on the performance of the aeroelastic belt. In the diagram, it is clear that locating the device at the leeward side of the roof will result in little to no energy generation due to the low wind speeds in this area. However, it should be noted that this may

not be the case for other wind angle. Therefore, location surveying and wind assessment are very important when installing devices in buildings. At wind velocity (U_H) 4.7 m/s and 0° wind direction, the speed in R1 was the highest at 4.5 m/s while the lowest was observed for the R2 (centre of the roof).

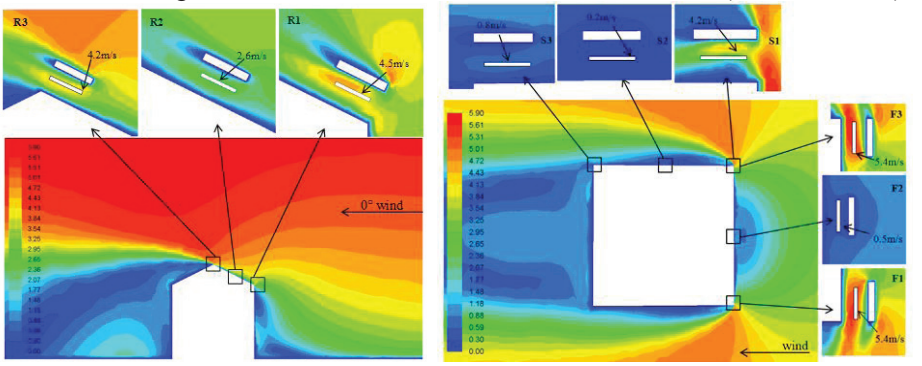

Fig. 3. Contours of velocity magnitude showing a cross-sectional (a) side view of the building and (b) top view of the building

Fig. 3b displays the velocity contours of a top view cross-sectional plane inside the computational domain. The approach wind profile entered from the right side of the domain and the airflow slowed down as it approached the building and accelerated as it flowed around the corners. Zoomed in views of the velocity distribution around the aeroelastic belt F1-F3 and S1-S3 are shown on top and right side of the diagram. At wind velocity (U_H) 4.7 m/s and 0° wind direction, the airflow speed in F1 and F3 were the highest at 5.4 m/s while the lowest was observed for the S2 and F2 located in recirculation zones.

Fig. 4a compares the estimated output of the device at various locations and wind directions (0, 45 and 90˚) while maintaining a uniform outdoor wind velocity. Refer to Fig. 1a for a clearer perspective. As observed, the highest power output comes from location R3 – the apex of the building – with an estimated output of 70 mw, resulting from wind speed that accelerated to approximately 7 m/s. This happens for an incoming wind that is directed 45 degrees relative to the building. Speed-up maximization occurs at this location.

Secondary to the building apex, locations on the edge also provide well above-average power output. Locations S3, F1 and R1 (in that order) make it to the priority choices for building integration of the aeroelastic belt, considering the power averages for 0, 45 and 90-degree orientations. The last locations an installer would want to situate an aeroelastic belt on are the central areas of the building's faces (illustrated by F2 and S2). Taking into account angular averages these locations provide the least amount of power, with no power generated at all for some cases due to the wind speed not being able to fulfil the aeroelastic belt's cut-in wind speed for generation. This finding can be considered by some to be a counterintuitive result, considering these locations are directly hit by the oncoming wind.

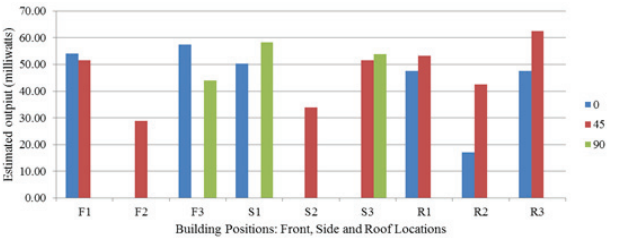

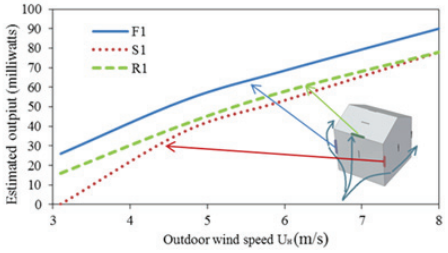

Fig. 4. (a) Estimated output of the aero-elastic belt based on the location and wind direction; (b) Impact of various outdoor wind speeds (U_H) on the estimated output of the aero-elastic belt for locations F1, S1 and R1.

Fig. 4b compares the estimated output of the device located in the three locations F1, S1 and R1 at various outdoor wind speeds. Among these three locations, at 0° wind direction, F1 provided the highest output ranging between 26 to 90 mW, while S1 showed the lowest output and only started to generate at outdoor wind velocity (UH) of 4.7 m/s. Further analysis of several points, if not all, involving various outdoor wind velocities can be performed to provide a more extended viewpoint.

5. Conclusions and Future Work

The aeroelastic belt is beneficial for low-energy wind harvesting in the built environment due to its low cost and modularity. The review of previous works on the aeroelastic belt showed that several authors have assessed the performance of the device in uniform flows in the laboratory but did not investigate the effect of buildings on its performance. Therefore, the current work addressed the issue by carrying out detailed CFD modelling. The work investigated the effect of various wind speeds and aeroelastic belt locations on the performance. The results of the flow around the buildings and pressure coefficients were validated with previous experimental work. The study utilised regression analysis and experimental data to estimate the power output. In terms of potential for power generation from the aeroelastic belt, the apex of the roof or the highest point of the building recorded the highest power yield, with this location's production being the largest with the 45-degree approach of the wind relative to the building. Intelligent placement of the aeroelastic belt would mean prioritizing the roof and the trailing edges of the building, and not the leading edge nor centres of surfaces, to yield the highest possible power generation.

There is a potential for further scaling up the system in terms of size and configuration, with the plausibility of constructing an array of aeroelastic belts. The results showed the importance of using detailed CFD analysis to evaluate the aeroelastic belt. The results showed the capabilities of CFD on assessing the optimum location of the devices around buildings. The modelling procedure and data presented in this work can be used to further investigate the urban integration of the aeroelastic belt.

Acknowledgement

We would like to thank British Council (DOST-Newton Fund no.209559487) for the funding of this research.

References

[1] Pérez-Lombard, L., Ortiz, J. and Pout, C. (2008) A review on buildings energy consumption information. Energy and Buildings. 40, 394-398.
[2] Toja-Silva, F., Lopez-Garcia, O., Peralta, C., Navarro, J. and Cruz, I. (2016) An empirical–heuristic optimization of the building-roof geometry for urban wind energy exploitation on high-rise buildings. Applied Energy. 164 769-794.
[3] Pimentel, D., Musilek P., Knight, A., and Heckenbergerova, J. (2010) Characterization of a wind flutter generator9th International Conference on Environment and Electrical Engineering, 81-84. IEEE.
[4] Arroyo, E., Foong, S., Maréchal and L., Wood, K.L. (2014) Experimental Study of an Omni-directional Wind Fluttering Energy Harvester. ASME 2014 Dynamic Systems and Control Conference.
[5] Ramasur D. and Hancke G.P. (2012) A wind energy harvester for low power wireless sensor networks. Proceedings of the IEEE International Instrumentation and Measurement Technology Conference (I2MTC '12), 2623–2627.
[6] Fei, F., Zhou, S., Mai, J. and Li, W. (2014) Development of an Indoor Airflow Energy Harvesting System for Building Environment Monitoring. Energies, 7, 2985-3003.
[7] Frayne, S. (2009) Generator utilizing fluid-induced oscillations. US7573143 B2.
[8] Sofotasiou, P., Calautit, J.K., Hughes, B.R. and O'Connor, D. (2016) Towards an integrated computational method to determine internal spaces for optimum environmental conditions. Computers & Fluids, 127, 146-160.
[9] Tominaga, Y., Akabayashi, S., Kitahara, T. and Arinami, Y. (2015) Air flow around isolated gable-roof buildings with different roof pitches: Wind tunnel experiments and CFD simulations, Building and Environment, 84, 204–213.

Biography

The author is a current PhD researcher for the Energy 2050 group in the University of Sheffield, United Kingdom. He is interested in new and emerging wind energy innovations. A big science advocate, once in a while he also makes time for sports, hiking and volunteering.